



ASSESSMENT OF THE IMPACT OF LAND USE/COVER DYNAMICITY ON THE LAND SURFACE TEMPERATURE OF CHHOTA RANGIT RIVER BASIN, IN DARJEELING HIMALAYA USING REMOTE SENSING AND GIS

Kabita Lepcha¹ and Sujit Mandal²

¹Assistant Professor, Dept. of Geography, University of Gour Banga.

²Professor, Dept. of Geography, Diamond Harbour Women's University .

ABSTRACT :

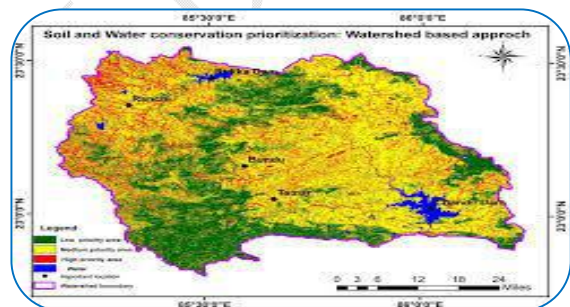
The land surface temperature changes due to drastic and continues land use/cover changes in the recent time is one of the imperative problems faced by not only the urban areas but also by the rural areas around the world. The continues process of land modifications mostly through the alteration of vegetation and water bodies into the impervious surfaces such as settlements, roads and other concrete structures etc; are playing a crucial role in changing the land surface characterises and related land surface temperature changes. The present paper thus focuses on the land-use/cover dynamicity and its impact on the land surface temperature of Chhota Rangit river basin in Darjeeling Hill during the period of 2001 and 2017. The land use/cover (LU/LC) map for the year 2001(Landsat-5) and 2017(Landsat-8 OLI) has been prepared using supervised classification techniques (maximum likelihood method) within Arc GIS 10.3.1 software. The Seasonal and temporal land surface emissivity and land surface temperature of the Chhota Rangit river basin is extracted for the phases of 2001 and 2017 from the satellite images (Landsat-5) and (Landsat-8 OLI). Air temperature map of Chhota Rangit river basin is also prepared for the estimation of temperature gap between land surface temperature and air temperature. The estimated average temperature gap in the study area during 2001 and 2017 is 8.54°C and 14.61°C and strongly determined by the existing land use and land cover pattern. There exists a strong negative correlation between NDVI and land surface temperature of Chhota rangit river basin. From the analysis, it is clear that the land surface temperature of the river basin has changed along with the changes of land use/cover during the period of 2001 to 2017.

KEYWORDS : Land use/cover, land surface temperature, land surface emissivity, Temperature Gap

1. INTRODUCTION

Land surface temperature is an important environmental factor which plays an important role in characterizing energy exchange of the Earth's surface and the atmosphere (Quattrochi and Luvall, 1999; Weng, 2009), it is basically the earth crust temperature where the sun's radiation is absorbed, reflected and refracted directly (Jeevalakshmi et al., 2017). However, the land surface temperature is highly determined

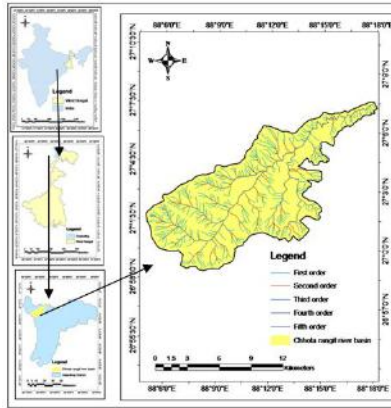
by the land use/cover characteristics, surface air temperature and soil moisture characteristics of the area. In the present time due to continues process of land use and land cover changes, such as the replacement of the vegetated areas by the urban expansion, conversion of the wetlands into settlement areas etc; has modified the physical properties of land surface, due to which the heat capacity, albedo, moisture content, conductivity, emissivity,



evapotranspiration etc; of the land surface has drastically changed, (Shoshany et. al., 1994; Friedl, 2002; Streutker, 2002; Chudnovsky et. al., 2004) which has resulted in changes of land surface temperature of an area. Such surface temperature changes due to drastic and continues land use and land cover changes is one the imperative problems faced by many rural and urban areas in the recent times. However, many studies are also being conducted around the world regarding the land surface temperature changes of various places. The Land surface temperature (LST) can be estimated with the help of the application of numerous environmental and socio-economic factors such as , land use and land cover (LULC) type and change, normalized difference vegetation index (NDVI), geometry of street canyon, intensity of human activity, population density and distribution, impervious surface abundance, etc (Eliasson, 1996; Elvidge et al., 1997; Bottyán and Unger, 2003; Yuan and Bauer, 2007; Weng et al., 2011; Li et al., 2011). However, the application of remote sensing and GIS has provided a great platform in the analysis of land surface temperature in the recent times. The different Remote sensing and GIS data like the thermal infrared (TIR) remote sensing images Spectro radiometer (MODIS) Landsat, Thematic Mapper (TM) and Enhanced Thematic Mapper Plus (ETM+), and Advanced Space borne Thermal Emission and Reflection Radiometer (ASTER)) etc; have been widely used by the scholars around the world for analysing the surface temperature of urban climate and environments (Streutker, 2003; Nichol, 1994, 2005; Lu and Weng, 2006; Weng, 2009). In India, a number of studies have also been conducted to analyse the urban heat island and land surface temperature especially for some metropolitan cities like Delhi by Mallick et al., (2008); Grover and Singh, (2015); Jaipur by Jalan and Sharma, (2014), Mumbai by Grover and Singh, (2015), Chennai by Lilly Rose and Devadas, (2009) Hyderabad city by Kumar et al. (2012), Dindigul drought prone district of Tamil Nadu by Rajeshwari and Mani (2014), English bazaar in Malda district by Ziaul and Pal (2016). Most of these studies are focused on the land surface temperature changes of the urban areas. However, the land surface temperature change due to the land use/cover changes is also an important problem faced by many rural areas as well. So the present paper is an attempt to analyse the impact of land use/cover dynamicity on the land surface temperature of Chhota Rangit river basin, in Darjeeling Himalaya, India using remote sensing and GIS. The objective of this paper is to study the Land surface temperature change in relation to the land use/land cover dynamicity basically in the Chhota Rangit river basin which is mostly rural in its characteristics. The main thrust of this paper is to see the land surface temperature and air temperature characteristics in different land use/ cover pattern like vegetation zones, settlement zones and water bodies during the selected time phases.

2. LOCATION OF THE STUDY AREA

The Chhota Rangit river basin is located between 26° 57' 0" N to 27° 20' 0" N and 88° 6' 0" E to 88° 18' 0" E in the district of Darjeeling, in West Bengal India. Total geographical area of the river basin is 140.98 sq km, which includes the maximum parts of the Darjeeling Pulbazar and Jorebunglow Sukiapokhari block. The area is drained by the Chhota Rangit River originating from the area below Tanglu in Singalila range on the Nepal border and its tributaries like Kahel khola, Hospital jhora, Relling khola, Serjan and Neora Jhora. The annual average rainfall and temperature of the study area is about 2547mm and 13.6°C respectively. The river basin in the recent times is experiencing drastic changes in its land use and land cover as a result of population growth, as well as due to the changes in socio economic status of people living in the river basin.



Map: 1: Location of study area

3. MATERIALS AND METHODS

For the completion of the present paper, various data like Topographical map 74 A/4, prepared by survey of India, LANDSAT TM data for 2001 and LANDSAT 8 OLI for 2017, obtained from the US Geological Survey (USGS) Global Visualization Viewer have been used. All data were at first registered into the UTM projection northern zone 45 datum WGS 84. The cloud cover has been removed from the satellite images using spatial analyst Tool, within Arc GIS 10.3.1 environment. The drainage basin map has been prepared from Toposheet map (74 A/4) prepared by Survey of India. LANDSAT TM data for 2001 and LANDSAT 8 OLI 2017 have been obtained from the US Geological Survey (USGS) Global Visualization Viewer. Arc GIS 10.3.1 and ERDAS IMAGINE 9.2 software have been used for the entire study. For extracting surface temperature from thermal band of Landsat imageries (Landsat-5 and Landsat-8), following steps have been followed.

3.1 LST extraction from thermal band

LST extraction from thermal band (Landsat-5)

The three steps were followed to derive the surface temperature from Landsat TM 5 Image (Band-6). Spectral radiance was calculated using following equation (Landsat Project Science Office, 2002):

Conversion of the digital number to spectral radiance

$$L = ((LMAX - LMIN) / (QCALMAX - QCALMIN)) * (QCAL - QCALMIN) + LMIN.....(Equation-1)$$

Where

LMAX= 15.303 and LMIN= 1.238

QCALMAX = 255 and QCALMIN = 1

QCAL= Digital number.

Conversion of spectral radiance to At-satellite brightness temperatures in Kelvin

$$TB = K2 / \ln [(K1/L \lambda) + 1]..... (Equation-2)$$

Where

K1= Calibration Constant 1 (607.76)

K2 = Calibration Constant 2 (1260.56) for the thermal band of the TM data and

TB = satellite brightness temperatures.

LST extraction from thermal band (Landsat-8)

Land Surface temperature from Landsat 8 TIRS was derived using band 10 and 11 following steps (LSDS-1574 version-2, 2016):

Conversion of the digital number to spectral radiance

TOA spectral radiance (L λ) = MLQCAL+AL..... (Equation-3)

Where

ML = Radiance multiplier

QCAL = Digital number

AL = Radian add

Table: 1 (Radiance multiplier)

Thermal constant	Band- 10	Band-11
Radiance multiplier	0.0003342	0.0003342
Radiance add	0.1	0.1
K1	774.89	480.89
K2	1321.08	1201.14

Conversion of spectral radiance to At-satellite brightness temperatures in Kelvin

TB = K2/ln [(K1/L λ) + 1]..... (Equation-4)

Where

K1= Calibration Constant 1

K2 = Calibration Constant 2 for the thermal band of the TM data and

TB = satellite brightness temperatures

Land surface temperature (LST)

The emissivity corrected land surface temperatures (St) have been computed following Artis and Carnahan (1982).

LST = TB / {(1+ λ * TB/ ρ) * ln (ϵ)}..... (Equation- 5)

Where

St = land surface temperature (LST) in Kelvin

λ = wavelength of emitted radiance in meters (for which the peak response and the average of the limiting wavelengths (λ = 11.5 μ m) (Markham and Barker, 1985) is used ρ = h * c/r (1.438 * 10⁻²m K), r = Boltzmann Constant (1.38 * 10⁻²³ J/K), h = Planck’s constant (6.626 * 10⁻³⁴ J s), and c = velocity of light (2.998* 10⁸m/s) and ϵ = emissivity (ranges between 0.97 and 0.99) (Equation- 6).

Land surface emissivity(ϵ) = 0.004*Pv + 0.986(Equation- 6)

Where proportion of vegetation (Pv) can be calculated (Equation- 7)

$$Pv = \left(\frac{NDVI_r - NDVI_{min}}{NDVI_{max} - NDVI_{min}} \right)^2$$
 (Equation- 7)

Conversion of LST from Kelvin to degree Celsius

For the convenient of comprehension, the above derived LSTs’ unit was converted to degree Celsius using the relation of 0^oC equals 273.15 K.

3.2. Methods for framing used data layers

NDVI (Normalized Differences Vegetation Index), Normalized Differences Water Index (NDWI) and Normalized Differences Built up Index (NDBI) data layers were prepared from Landsat-5 and Landsat-8 satellite image are used for intra land use Land Surface Temperature change.

For NDVI extraction, method of Townshend and Justice (1986) has been used.

$$NDVI = \frac{(IRband - Rband)}{(IRband + Rband)}$$

Where,

IR = near infrared band (band 4 of TM and band 5 of OLI),

R = red band (TM band 3 and OLI band 4)

For extracting NDWI, equation framed by McFeeters (1996) is used:

$$NDWI = \frac{(Greenband - Nirband)}{(Greenband + Nirband)}$$

Where, Green is the green band (TM band 2 and OLI Band 3) and NIR is the near infrared band (Band 5 of OLI, band 4 of TM).

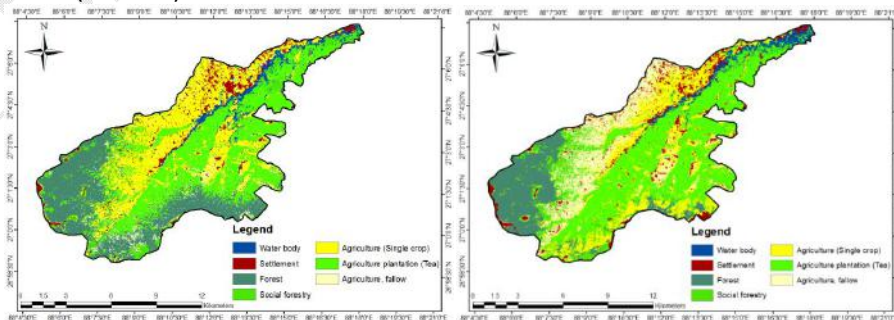
Normalized differential built up index (NDBI) has been calculated following Zha et al. (2003).

$$NDBI = \frac{(MIR - NIR)}{(MIR + NIR)}$$

Where, MIR is the middle infrared band (TM band 5, OLI band 6) and, NIR is the near infrared band (TM band 4, OLI band 5).

4. Land Use And Land Cover Classification

Land use data set for the Chhota Rangit river basin has been prepared from Landsat-5 and Landsat-8 imageries. Supervised classification techniques (non parametric rule: maximum likelihood) has been used for land use land cover (LULC) classification. The spatial pattern and distribution of land use and land cover in the study area are shown in (Map: 2 and 3). The land use and land cover of the Chhota Rangit river basin has been classified into seven classes such as; water bodies, settlement, forest, social forestry, agriculture (single crop), plantation (Tea), and agriculture/ fallow. The area covered by the settlement in 2001 was 4.22% which rose to 6.02% in 2017. Similarly the area covered by agriculture, fallow land, social forestry, water bodies, and plantation were 25.91%, 4.90%, 5.81%, 4.54%, 30.49% in 2001 and significantly changed in 2017, which was 18.38%, 15.02%, 12.45%, 3.30% and 30.42% respectively. The forest area and water bodies in the study area have continuously decreased during the period of 2001 to 2017, whereas the area under settlement has drastically increased (Table: 2).



Map: 2 (LU/LC, 2001)

Map: 3 (LU/LC, 2017)

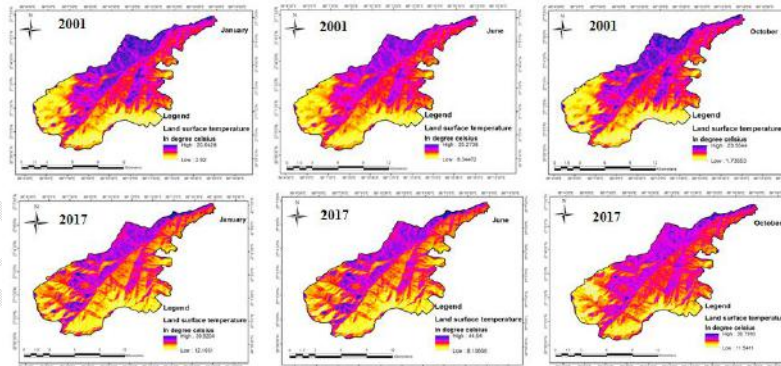
Table 2: Land use/land cover classes in Chhota Rangit river basin

Land use/land cover classes	Area			
	2001		2017	
	Area inkm ²	% of area	Area inkm ²	% of area
Water bodies	6.40	4.54	4.66	3.30
Settlement	5.95	4.22	8.49	6.02
Forest	34.21	24.26	20.27	14.38
Social forestry	8.19	5.81	17.55	12.45
Agriculture (Single crop)	36.31	25.75	25.91	18.38
Agriculture plantation (Tea)	42.98	30.49	42.88	30.42
Agriculture, Fallow	6.915	4.90	21.18	15.02
Total	140.98	100	140.98	100

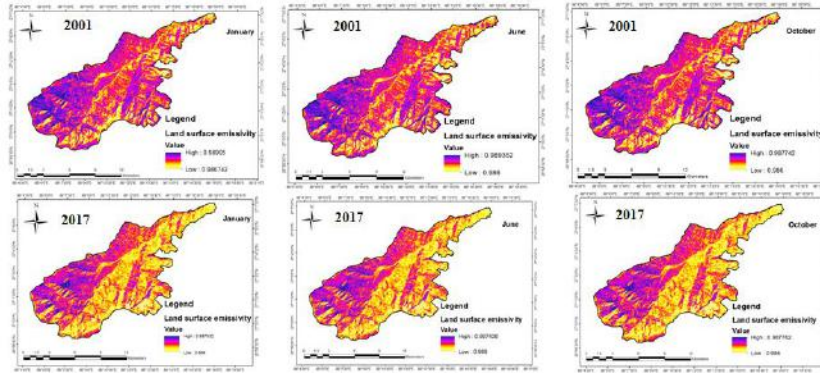
4. RESULTS AND ANALYSIS

4.1. Land surface temperature change

Spatial pattern of land surface temperature for 2001 and 2017 has been shown in Map 4. Land surface temperature in the study area during the month of January 2017 ranged from 12.10^oc to 39.52^oc, which was 2.92^oc to 20.04^oc during January 2001. Maximum LST of June and October in 2001 and 2017 has also risen from 25.27^oc to 44.54^oc and 23.55^oc to 36.79^oc. The average land surface temperature of Chhota Rangit river basin in January, June and October 2001 were 11.48^oc, 16.80^oc and 12.64^oc and the average land surface temperature in January, June and October 2017 were 25.81^oc, 26.32^oc and 24.16^oc which shows an increase in the land surface temperature. Seasonal Land surface emissivity in the study area for 2001 January, June and October was (0.986742 to 0.988905), (0.986 to 0.98935) and (0.986 to 0.987742) respectively. However, the seasonal Land surface emissivity for the same months in the year of 2017 were (0.986 to 0.987032), (0.986 to 0.987438) and (0.986 to 0.987782) (Map 5). It is clear from the analysis that the land surface temperature for the overall land use and land cover in the study area for the months of January, June and October has increased during the period of 2001 to 2017.



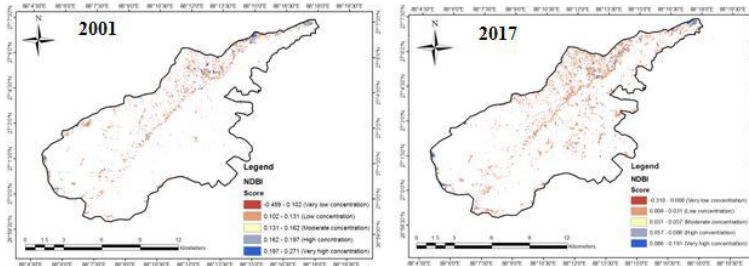
Map: 4 (Land surface temperature in 2001 to 2017)



Map: 5 (Land surface emissivity in 2001 to 2017)

4.2. Land surface temperature change in Settlement areas

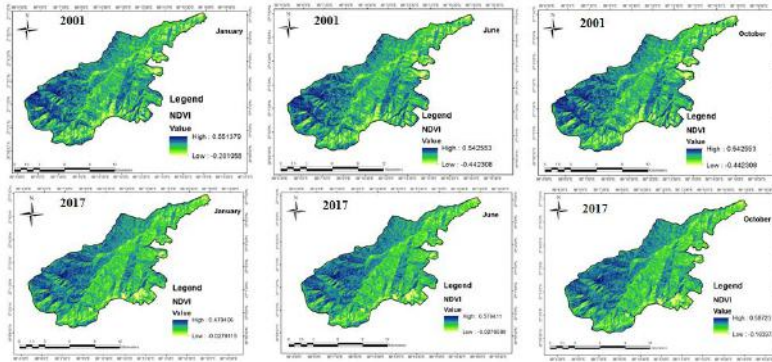
High land surface temperatures are mostly related with the built up areas and densely populated areas (Xiong et al. 2012). The Normalized Differentiated Build up Index (NDBI) classes indicates the intensity and spatial pattern of settlement area for the period of 2001 and 2017. The NDBI value in the study area ranges between -0.459 to 0.271 in 2001 and -0.310 to 0.191 in 2017 (Map: 6). It is observed from the analysis that the Land surface temperature is closely related with NDBI value. High land surface temperature is mostly found in the places where the intensity of settlement is also very high. It can be said that in the Chhota Rangit river basin both the NDBI and land surface temperature has simultaneously increased during the period of 2001 and 2017.



Map: 6 (NDBI score in 2001 to 2017)

4.3. Land surface temperature change in Vegetation area

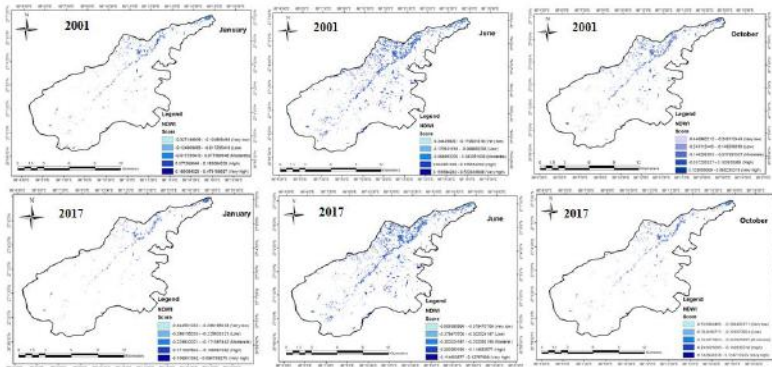
Low vegetation cover is associated with urban heat island effect (Weng and Yang 2004). The NDVI classes indicate the spatial pattern and density of vegetation since 2001 and 2017 (map: 7). The classification has been done for creating a relationship between NDVI of various densities and the land surface temperature of the river basin. It can be said that higher level of land surface temperature in the Chhota Rangit river basin is associated with lower NDVI level. NDVI value of the river basin ranges -0.201058 to 0.551379 (January), -0.442308 to 0.542553 (June), -0.384615 to 0.571429 (October) in 2001 and -0.2079115 to 0.479406 (January), -0.0276589 to 0.579411 (June), -0.103973 to 0.53723 (October) in 2017.



Map: 7 (NDVI score in 2001 to 2017)

4.4. Land surface temperature change in Water bodies

Land surface temperature is influenced by the water bodies. Temperature of water is lower than the other type of land use and land covers (Hathway and Sharples, 2012; Zhang and Huang, 2015). The NDWI classes indicate the spatial pattern and quality of water bodies in different season for 2001 and 2017 (map: 8). From these maps, it is clear that the extension of water bodies in the study area has decreased in every summer months, lowering the NDWI score for the river basin. The decrease in the areas covered by water bodies in the study area indicates the simultaneous increase in the land surface temperature in the river basin.



Map: 8 (NDWI score in 2001 to 2017)

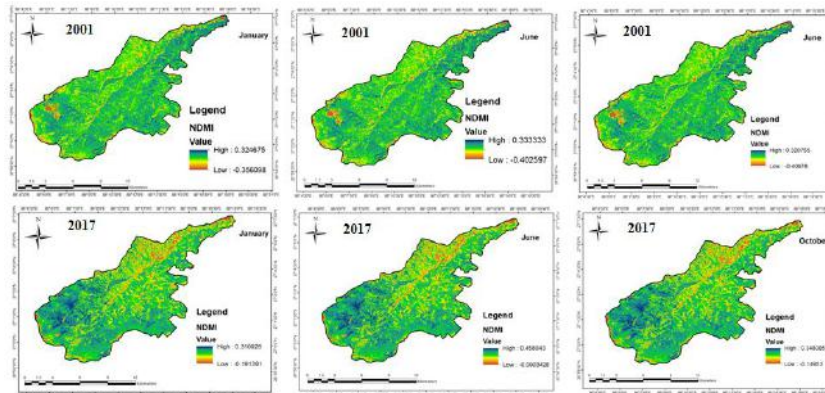
4.5. Normalized Difference Moisture Index

Normalized Difference Moisture Index of the river basin has been prepared using the equation (10). This Normalized Difference Moisture Index (NDMI) was developed by Wilson and Sader, (2002). NDMI is closely related with NDVI and both are inversely related with land surface temperature (Sahu, 2014). Negative NDMI indicates low moisture content and positive NDMI indicates high moisture content of the river basin (Duran, 2015). In this work, it is found that low surface temperature is found in the place where NDMI is very high. So, it can be said that NDMI is negatively related with land surface temperature. NDMI value of the river basin ranges -0.356098 to 0.324675 (January), -0.402597 to 0.333333 (June), --0.40678 to 0.3220755 (October) in 2001 and -0.191391 to 0.310926 (January), -0.0903428 to 0.458043 (June), -0.14953 to 0.348085 (October) in 2017 (map: 9).

$$NDMI = \frac{(NIR - SWIR)}{(NIR + SWIR)} \dots\dots\dots (Equation- 10)$$

Where,

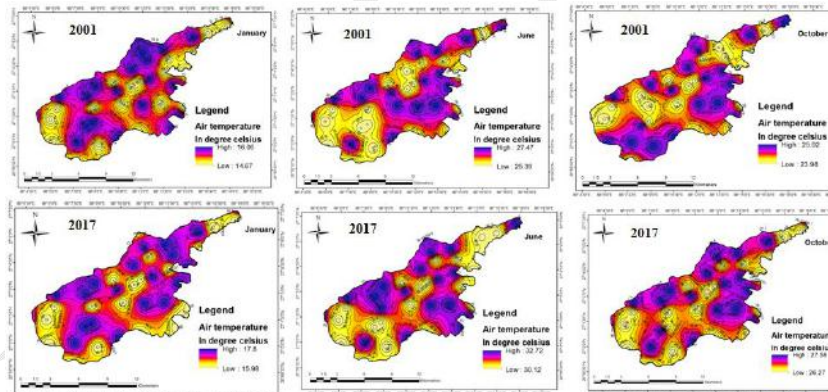
In Landsat 4-7, NIR is band no 4 and SWIR is band no 5.
In Landsat 8, NIR is band no 5 and SWIR is band no 6.



Map: 9 (NDMI score in 2001 to 2017)

4.6. Spatial aerial temperature pattern

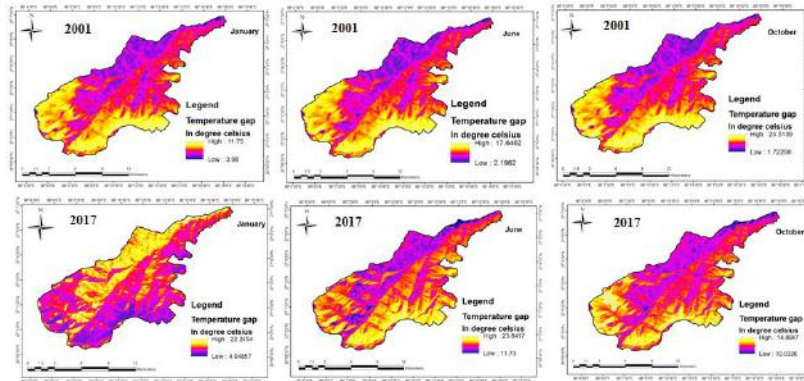
Spatial air temperature maps have been prepared to see the relationship between air temperature and land surface temperature in different season for 2001 and 2017. Minimum air temperature in January, June and October during 2001 were 14.67°C , 25.39°C and 23.98°C while maximum air temperature in January, June and October 2017 were 16.06°C , 27.47°C and 25.92°C . Maximum air temperature in January, June and October 2017 were 17.8°C , 32.72°C and 27.58°C (map: 10). From the result, it is clear that the spatial mean air temperature in the study area has also changed during the period of 2001 to 2017.



Map: 10 (Spatial air temperature in 2001 to 2017)

4.7. Temperature gap between air temperature and LST since 2001 to 2017

Spatial temperature gap between air and land surface temperature in the study area has been shown for the months of January, June, October 2001 and 2017 respectively (Map: 11). Spatial temperature gap maps are prepared to see whether the temperature gap has increased or decreased during the period of 2001 to 2017. Average temperature gap in 2001 was 8.54°C and in 2017 it was 14.61°C . From the result, it is evident that the temperature gap between the air temperature and land surface temperature has increased over the period in the Chhota Rangit river basin. Seasonal temperature gap in the study area for January, June and October 2001 was (3.98°C to 11.75°C), (2.19°C to 17.64°C) and (3.98°C to 11.75°C) respectively. However, the seasonal temperature gap for January, June and October 2017 were (4.64°C to 22.54°C), (11.73°C to 23.84°C) and (10.03°C to 14.88°C). Thus there has been an increase in the seasonal temperature gap also in the river basin during 2001 and 2011.



Map : 11 (Temperature gap in 2001 to 2017)

4.8. Land surface temperature in different land use and land cover area

Seasonal land surface temperature is measured in different land use and land cover area of the Chhota Rangit river basin using Arc GIS 10.3.1 software environment. From the results, it is clear that the high land surface temperature is found in the build-up areas (January- 39.05^oc, June- 44.12^oc and October- 36.19^oc in 2017) and low in forest cover area (January- 2.97^oc, June- 8.27^oc and October- 1.65^oc in 2017). The average land surface temperature in 2001 and 2017 in each land use and land cover areas has been shown in (Table: 3). It can be said that high land surface temperature is found profoundly in the build up areas than the other kind of land use and land cover.

Table.3: Land surface temperature in different land use/land cover

Land use/land cover classes	Average land surface temperature in degree Celsius					
	2001			2017		
	January	June	October	January	June	October
Water bodies	9.12	12.34	11.79	14.59	15.29	14.75
Settlement	20.02	25.12	23.25	39.05	44.18	36.19
Forest	2.97	8.27	1.65	11.12	12.87	11.34
Social forestry	12.36	8.27	13.27	17.21	18.74	17.45
Agriculture (Single crop)	16.92	14.82	17.38	20.77	25.31	23.77
Agriculture plantation (Tea)	16.78	17.89	16.98	21.37	25.98	24.12
Agriculture, Fallow	17.31	17.21	17.45	21.95	25.57	23.98

5. CONCLUSION

The land surface temperature change due to rampant land cover modifications is the widely accepted fact at the present time. The present paper is an attempt to examine the land-use/cover dynamicity and its impact on the land surface temperature of the Chhota Rangit River basin, which is basically rural in characteristics during the 2001 and 2017. From the detail analysis and the derived results, it can be said that the land surface temperature in the study area has been significantly increased during the period of 2001 to 2017. The land surface temperature has a negative relation with the elevation and a positive relation with the build up area because the high land surface temperature is found in the places where the intensity of NDBI is very high. The temperature gap between land surface temperature and air temperature has also increased from 2001 to 2017. Spatial mean air temperature has increased by 0.99^oc in the study area. In the conclusion it can be said that the variation of the land surface temperature is highly determined by the land use and land cover types and changes. Further it can be said that the land surface temperature of the Chhota Rangit river basin has changed over the time as a result of continuous land use and land cover changes in the river basin.

Carson et al., 1994; Gillies & Carlson, 1995; Gillies et al., 1997

REFERENCE

1. Artis, D.A., and Carnahan, W.H., (1982): "Survey of emissivity variability in thermography of urban areas". *Remote Sensing Environment*, Vol. 12, pp. 313–329.
2. Bottyán, Z., and Unger, J., (2003): "A multiple linear statistical model for estimating the mean maximum urban heat island". *Theoretical and Applied Climatology*, Vol. 75 (3–4), pp. 233–243.
3. Chudnovsky, A., Ben-Dor, E., and Saaroni, H., (2004): "Diurnal thermal behavior of selected objects using remote sensing measurements". *Energy and Buildings*, Vol. 36, pp. 1063–1074.
4. Duran, C., (2015): "Effects on drought and vegetation of topography in the Tarsus River Basin (Southern Turkey)". *International Journal of Human Sciences*, Vol. 12 (2), pp. 1853–1866. <http://dx.doi.org/10.14687/ijhs.v12i2.3370>.
5. Eliasson, I., (1996): "Urban nocturnal temperatures, street geometry and land use". *Atmospheric Environment*, Vol. 30 (3), pp. 379–392.
6. Elvidge, C.D., Baugh, K.E., Kihn, E.A., Kroehl, H.W., Davis, E.R., Davis, C.W., (1997): "Relation between satellite observed visible-near infrared emissions, population, economic activity and electric power consumption". *International Journal of Remote Sensing*, Vol. 18 (6), pp. 1373–1379.
7. Friedl, M., (2002): "Forward and inverse modeling of land surface energy balance using surface temperature measurements". *Remote Sensing of Environment*, Vol. 79 (2), pp. 344–354.
8. Grover, A., and Singh, R.B. (2015): "Analysis of Urban Heat Island (UHI) in Relation to Normalized Difference Vegetation Index (NDVI): a Comparative Study of Delhi and Mumbai". *Environments*, Vol. 2, pp. 125–138.
9. Hathway, E.A. and Sharples, S. (2012): "The interaction of rivers and urban form in mitigating the Urban Heat Island effect: a UK case study". *Build. Environment*, Vol. 58, pp. 14–22.
10. Jalan, S. And Sharma, K. (2014): "Spatio-Temporal Assessment of Land Use/Land Cover Dynamics and Urban Heat Island of Jaipur City Using Satellite Data". *Int. Arch. Photogramm., Remote Sens. Spatial Inform. Sci.* XL-8, pp. 767–772.
11. Jeevalakshmi. D, Reddy. S. N., and Manikian. B., (2017): "Land Surface Temperature Retrieval from LANDSAT data using Emissivity Estimation". *International Journal of Applied Engineering Research*, Vol. 12 (20), pp. 9679-9687.
12. Kumar K.S, Bhaskar P.U, and Padmakumari. K. (2012): "Estimation of land surface temperature to study urban heat Island effect using Landsat ETM+ Image". *Int J EngScTechnol*, Vol. 4(2), pp. 771–778.
13. Landsat Project Science Office (2002): "Landsat 7 Science Data User's Handbook". URL: http://ltpwww.gsfc.nasa.gov/IAS/handbook/handbook_toc.html, Goddard Space Flight Center, NASA, Washington, DC (last date accessed: 10 September 2003).
14. Lilly Rose, A. and Devadas, M.D. (2009): "Analysis of Land Surface Temperature and Land Use/Land Cover Types Using Remote Sensing Imagery - A Case in Chennai City, India". The seventh International Conference on Urban Climate., held on 29 June – 3 July 2009, Yokohama, Japan
15. Li, J., Song, C., Cao, L., Zhu, F., Meng, X., and Wu, J., (2011): "Impacts of landscape structure on surface urban heat islands: a case study of Shanghai, China". *Remote Sensing of Environment*, Vol. 115, pp. 3249–3263.
16. Landsat-1574 version-2 (2016): "Landsat 8 (L8) Data Users Handbook". URL: <https://landsat.usgs.gov/sites/default/files/documents/Landsat8DataUsersHandbook.pdf>. Approved by K. Zaner, Landsat CCB chair USGS (March 29, 2016).
17. Lu, D., Weng, Q., (2006): "Spectral mixture analysis of ASTER imagery for examining the relationship between thermal features and biophysical descriptors in Indianapolis, Indiana". *Remote Sensing of Environment*, Vol. 104 (2), pp. 157–167.
18. Mallick, J., Kant, Y. And Bharath, B.D. (2008): "Estimation of land surface temperature over Delhi using Landsat-7 ETM+". *J. Ind. Geophys. Union*, Vol. 12 (3), pp. 131–140.

19. Markham, B.L., Barker, J.K., (1985): "Spectral characteristics of the LANDSAT Thematic Mapper sensors". *Int. J. Remote Sens.* Vol. 6, pp. 697–716.
20. McFeeters, S.K. (1996): "The use of normalized difference water index (NDWI) in the delineation of open water features". *Int. J. Remote Sensing*, Vol. 17 (7), pp. 1425–1432.
21. Mondall, and Bandyopadhyay J (2014): "Coastal zone mapping through geospatial technology for resource management of Indian Sundarban, West Bengal, India". *Int J Remote Sens Appl*, Vol. 4(2), pp.103–112.
22. Nichol, J.E., (1994): "A GIS based approach to microclimate monitoring in Singapore's high rise housing estates". *Photogrammetric Engineering and Remote Sensing*, Vol. 60(10), pp. 1225–1232.
23. Nichol, J.E., (2005): "Remote sensing of urban heat islands by day and night". *Photogrammetric Engineering and Remote Sensing*, Vol. 71 (5), pp. 613–621.
24. Quattrochi, D.A., Luvall, J.C., (1999): "Thermal infrared remote sensing for analysis of landscape ecological processes: methods and applications". *Landscape Ecology*, Vol.14, pp. 577–598.
25. Rajeshwari A, and Mani N.D (2014): "Estimation of land surface temperature of Dindigul district using Landsat 8 data". *Int J Res Eng Technology*, Vol. 3(5), pp. 122–126.
26. Sahu, A. S., (2014): "A Study on Moyna Basin Water-Logged Areas (India) Using Remote Sensing and GIS Methods and Their Contemporary Economic Significance". *Geography Journal*, Vol. 2014, pp. 1-9. Article ID 401324, <http://dx.doi.org/10.1155/2014/401324>
27. Shoshany, M., Aminov, R., Goldreich, Y., (1994): "The extraction of roof tops from thermal imagery for analyzing the urban heat island structure". *Geocarto International*, Vol. 4, pp. 61–69.
28. Streutker, D.R., (2002): "A remote sensing study of the urban heat island of Houston, Texas". *International Journal of Remote Sensing*, Vol. 23, pp. 2595–2608.
29. Streutker, D.R., (2003): "Satellite-measured growth of the urban heat island of Houston, Texas". *Remote Sensing of Environment*, Vol. 85 (3), pp. 282–289.
30. Townshend, J.R. and Justice, C.O. (1986): "Analysis of the dynamics of African vegetation using the normalized difference vegetation index". *Int. J. Remote Sensing*, Vol. 7 (11), pp. 1435–1445.
31. Weng, Q., and Yang, S. (2004): "Managing the adverse thermal effects of urban development in a densely populated Chinese city". *J. Environ. Management*, Vol. 70, pp. 145–156.
32. Weng, Q., Rajasekar, U., Hu, X., (2011): "Modeling urban heat islands and their relationship with impervious surface and vegetation abundance by using ASTER images". *IEEE Transactions on Geoscience and Remote Sensing*, Vol. 49, pp. 4080–4089.
33. Weng, Q., (2009): "Thermal infrared remote sensing for urban climate and environmental studies: methods, applications, and trends". *ISPRS Journal of Photogrammetry and Remote Sensing*, Vol. 64 (4), pp. 335–344.
34. Wilson, E. H. and Sader, S. A., (2002): "Detection of forest harvest type using multiple dates of Landsat TM imagery," *Remote Sensing of Environment*, vol. 80, no. 3, pp. 385–396.
35. Wu, C., (2009): "Quantifying high-resolution impervious surfaces using spectral mixture analysis". *International Journal of Remote Sensing*, Vol. 30 (11), pp. 2915–2932.
36. Xiong, Y., Huang, S., Chen, F., Ye, H., Wang, C. and Zhu, C. (2012): "The impacts of rapid urbanization on the thermal environment: a remote sensing study of Guangzhou, South China". *Remote Sensing*, Vol. 4, pp. 2033–2056.
37. Yuan, F., Bauer, M.E., (2007): "Comparison of impervious surface area and normalized difference vegetation index as indicators of surface urban heat island effects in Landsat imagery". *Remote Sensing of Environment*, Vol. 106, pp. 375–386.
38. Zha, Y., Gao, J. And Ni, S. (2003): "Use of normalized difference built-up index in automatically mapping urban areas from TM imagery". *Int. J. Remote Sens.*, Vol. 24 (3), pp. 583–594.
39. Zhang, W. And Huang, B. (2015): "Land use optimization for a rapidly urbanizing city with regard to local climate change: Shenzhen as a case study". *J. Urban Plan. Dev.* 141 (1). Article ID 05014007.

-
40. Ziaul. Sk, and Pal. S (2016): "Image based surface temperature extraction and trend detection in an urban area of West Bengal, INDIA". Journal of environmental geography, Vol. 9 (3-4), pp. 13-25.

LBP PUBLICATION